Accepted Manuscript

Comparisons of the spectroscopic and microbiological activities among coumarin-3-carboxylate, o-phenanthroline and zinc(II) complexes

María S. Islas, Juan J. Martínez Medina, Oscar E. Piro, Gustavo A. Echeverría, Evelina G. Ferrer, Patricia A.M. Williams

PII:	S1386-1425(18)30194-X
DOI:	doi:10.1016/j.saa.2018.03.003
Reference:	SAA 15875
To appear in:	*Spectrochimica Acta Part A: Molecular and Biomolecular Spectroscopy*
Received date:	27 December 2017
Revised date:	28 February 2018
Accepted date:	2 March 2018

Please cite this article as: María S. Islas, Juan J. Martínez Medina, Oscar E. Piro, Gustavo A. Echeverría, Evelina G. Ferrer, Patricia A.M. Williams , Comparisons of the spectroscopic and microbiological activities among coumarin-3-carboxylate, o-phenanthroline and zinc(II) complexes. The address for the corresponding author was captured as affiliation for all authors. Please check if appropriate. Saa(2017), doi:10.1016/j.saa.2018.03.003

Comparisons of the spectroscopic and microbiological activities among coumarin-3-carboxylate, o-phenanthroline and zinc(II) complexes.

María S. Islas[a], Juan J. Martínez Medina[b], Oscar E. Piro[c], Gustavo A. Echeverría,[c] Evelina G. Ferrer[a], Patricia A.M. Williams[a*]

[a]Centro de Química Inorgánica (CEQUINOR). FCE, UNLP, Bv. 120 nº 1465 (1900) La Plata, Argentina.

[b]Departamento de Química, UNCAUS, Cte. Fernández 755 (3700), Chaco, Argentina.

[c] Departamento de Física, Facultad de Ciencias Exactas, Universidad Nacional de La Plata and IFLP(CONICET, CCT La Plata), C.C. 67, 1900 La Plata, Argentina

[*]To whom correspondence should be addressed. E-mail: williams@quimica.unlp.edu.ar, tel/fax: 54 (0)221- 4454393

Keywords:

Coumarin-3-carboxylic acid; Zn complexes; Vibrational spectroscopy: NMR spectroscopy; Antimicrobial activities; behavior against alkaline phophatase.

Abstract

Coumarins (2H-chromen-2-one) are oxygen-containing heterocyclic compounds that belong to the benzopyranones family. In this work we have synthesized different coordination complexes with coumarin-3-carboxylic acid (HCCA), o-phenanthroline (phen) and zinc(II). In the reported $[Zn(CCA)_2(H_2O)_2]$ complex, coumarin-3-carboxylate (CCA) is acting as a bidentate ligand while in the two prepared complexes, $[Zn(phen)_3]CCA(NO_3)$ (obtained as a single crystal) and $[Zn(CCA)_2phen].4H_2O$, CCA is acting as a counterion of the complex cation $[Zn(phen)_3]^{+2}$ or coordinated to the metal center along with phen, respectively. These compounds were characterized on the basis of elemental analysis and thermogravimetry. NMR, FTIR and Raman spectroscopies of the compounds and the CCA potassium salt (KCCA) allow to determine several similarities and differences among them. Finally, their behavior against alkaline phosphatase enzyme and their antimicrobial activities were also measured.

Abbreviations

ALP	alkaline phosphatase
ATCC	American Type Culture Collections
CCA	coumarin-3-carboxylate
HCCA	coumarin-3-carboxylic acid
HSQC	heteronuclear single quantum coherence
KCCA	coumarin-3-carboxylate potassium salt
MIC	minimum inhibitory concentration
phen	o-phenanthroline

1. Introduction

Coumarins (2H-chromen-2-one) are oxygen-containing heterocyclic compounds that belong to the benzopyranones family and can be found mainly in plants. They have been associated with beneficial effects on human health, such as reducing the risk of cancer, diabetes, and cardiovascular diseases, among others. These effects are thought to be related to the radical scavenging effect, due to their antioxidant activities, along with other possible mechanisms, such as anti-inflammatory properties and interaction with several enzymes [1,2]. It is also well known that coumarin derivatives, such as coumarin-3-carboxylic acid (HCCA) can yield a wide variety of metal complexes with different coordination modes, spectroscopic properties, and potential applications (Scheme 1). The complexation of coumarin derived ligands to various metal ions established a promising route towards the development of new therapeutic agents [3,4]. For instance, an enhancement of antimicrobial activity of the silver(I)-HCCA coordination complex in comparison with the free ligand has previously been reported [5]. In addition, 1-10-phenanthroline (phen) metal complexes can also act as both, bacteriostatic and bactericidal compounds [6].

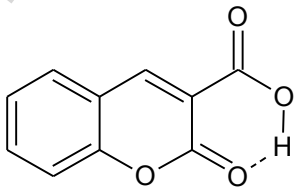

HCCA

Scheme 1. Structure of coumarin-3-carboxylic acid

Zinc is the second most abundant trace metal for humans, animals, plants and microorganisms after iron [7]. It is a multi-functional element that is found in almost 300 enzymes where it plays catalytic, co-catalytic, and/or structural functions [8]. A great degree of complexation is associated with zinc in biological systems. Hence, the most advantageous way to its biological

release in order to supply the free metal ion required for enzymatic synthesis facilitating Zn-dependent biochemical processes is the use of low molecular weight chelates or complexes of Zn [9].

In this paper, we have synthesized and studied two CCA containing complexes of zinc(II) and phen, $[Zn(phen)_3]CCA(NO_3).7H_2O$ (Znphen) and $[Zn(CCA)_2phen].4H_2O$ (ZnCCAphen). The spectroscopic properties of these coordination complexes and those of the reported binary complex $[Zn(CCA)_2(H_2O)_2]$ (ZnCCA) [10] were evaluated. The structure of Znphen has been solved by single crystal X-ray determinations. Besides, X-ray single-crystal structure analysis of the synthesized ZnCCA complex was found to be in good agreement with previously reported data [10].

Due to the presence of carbonyl and carboxylate groups in *cis*- position, coumarin-3-carboxylate (CCA) can act as a monodentate or bidentate ligand (through carboxylate moiety), or as a bidentate ligand (through both carboxylate and carbonyl groups). In the bibliography there has been some controversy in the assignment of the stretching modes of carbonyl and carboxyl groups because of their proximity, similarities, and the presence of an intramolecular bonding in HCCA [3,5]. Moreover, it has also been observed that the shifts of the C=O stretching frequencies are not a direct indication of a metal coordination to the corresponding groups when hydrogen bonds are present [11]. Herein, and through the experimental measurements of bond distances, we approach this problem studying their spectroscopic properties by comparing the different binary complexes where CCA acts as a bidentate ligand in one of them and as a counterion in the other. Although the spectral behavior of ZnCCA complex was already reported by Creaven et. al. [3], on the basis of the single crystal X-Ray diffraction determinations [10] and our own measurements, we show a different coordination mode of CCA, with the carboxylate and carbonyl moieties chelating the metal center (not with bidentate carboxylate coordination). The spectroscopic properties of the complexes have also been compared with a previously

synthesized potassium salt of CCA (KCCA). In addition, we have studied the properties of the ZnCCAphen complex, in which CCA shows similar coordination modes than ZnCCA.

We have systematically studied the spectroscopic patterns of these compounds comparing NMR in combination with FTIR and Raman spectra. Moreover, the antimicrobial activities and the behavior on alkaline phosphatase (ALP) have also been determined.

2. Materials and Methods

2.1. Instruments, Reagents and Materials

All chemicals $Zn(NO_3)_2.6H_2O$ (Merck), coumarin-3-carboxylic acid (Fluka) and o-phenanthroline dihydrate (Sigma) were of analytical grade and used without further purification. Elemental analyses for carbon, nitrogen and hydrogen were performed using a Carlo Erba EA 1108 analyzer. FTIR spectra of powdered samples (as pressed KBr pellets) were measured with an Equinox 55 FTIR-spectrophotometer from 4000 to 400 cm^{-1}. The dispersive Raman spectra were collected on a Horiba-Jobin-Yvon T64000 Raman spectrometer, with a confocal microscope (10x objective) and CCD detection. A Kr laser with 647.1 nm of excitation wavelength and 500mW power was used. Calibration was performed using the 459 cm^{-1} band of CCl_4. NMR spectra were acquired in a Bruker UltraShield 600 Plus, 14.1 Tesla with ^1H resonance of 600 MHz. Thermogravimetric measurement (TG) were performed on a Shimadzu system (model TG-50) working in an oxygen flow (50 mL min^{-1}) at a heating rate of 10 ^oC min^{-1}. Sample quantities ranged from 5 to 10 mg.

2.2. Synthesis of the complexes

Synthetic methods for both binary and ternary complexes, as well as the potassium salt are developed in this section.

KCCA: coumarin-3-carboxylic acid was dissolved in water at 60 ºC under continuous stirring. Then, the pH was adjusted to 9 by the addition of 1M KOH obtaining a light-yellow solution.

Finally, acetone was added until precipitation of KCCA. Elemental analysis calculated for $KC_{10}H_5O_4$ (228 g/mol): C, 52.6; H, 2.2. Found: C, 52.7; H, 2.3. The thermogravimetric analysis (Fig. S1) has shown a weight loss (79.4%, calc.; 79.0%, exp.) at 800 °C and represents the formation of K_2O (characterized by FTIR spectroscopy).

$[Zn(CCA)_2(H_2O)_2]$: Single crystals of the complex were obtained according to a recent literature procedure [10]. Briefly, a mixture of coumarin-3-carboxylic acid (0.1 mmol) and LiOH (0.2 mmol) in water (10 ml) was added in a test-tube. Then, a solution of $Zn(NO_3)_2$ (0.1 mmol) in ethanol (10 ml) was added on the top of the mixture by carefully layering. After about two months at room temperature, colorless single crystals suitable for X-ray determinations were obtained at the boundary between the ethanol solution and the water layer. Elemental analysis calculated for $ZnC_{20}H_{14}O_{10}$ (479.4 g/mol): C, 50.1; H, 2.9. Found: C, 50.0; H, 2.9. The thermogravimetric analysis (Fig. S2) confirmed the presence of two water molecules per zinc atom (Exp. loss: 7.7%. Calc. loss: 7.5%; broad endothermic peak, DTA, 182 °C). At 800 °C the weight loss (83.0%, calc.; 82.6%, exp.) represents the formation of ZnO that was characterized by FTIR spectroscopy.

$[Zn(CCA)_2phen].4H_2O$: HCCA (2 mmol in 10 ml of water) was dissolved under continuous stirring and pH was adjusted to 6 with NaOH 1M. Then, phen (2 mmol in 3 ml of ethanol) and $Zn(NO_3)_2$ (1 mmol in 2 ml of water) solutions were added to the previous colorless mixture. Immediately, a white precipitated was formed. The solid was filtered off, washed several times with water and dried in oven at 60 ºC. Elemental analysis calculated for $ZnC_{32}H_{26}N_2O_{12}$ (695.4 g/mol): C, 55.2; H, 3.7; N, 4.0. Found: C, 55.3; H, 3.7; N, 4.1. The thermogravimetric analysis (Fig. S3) confirmed the presence of four labile water molecules per zinc atom (Exp. loss: 10.4% Calc. loss: 10.3%; endothermic peaks, DTA, in three successive stages at 96 °C, 147 ºC and 168 ºC). At 800 °C the weight loss (88.3%, calc.; 88.4%, exp.) represents the formation of ZnO that was characterized by FTIR spectroscopy.

[Zn(phen)$_3$](CCA)(NO$_3$).7H$_2$O: HCCA (2 mmol) was dissolved in 10 ml of water and NaOH 1M was added to achieve a pH value of 6. Then an ethanolic solution of phen (1 mmol in 3 ml) and an aqueous solution of $Zn(NO_3)_2$ (1 mmol in 2 ml) were added. The final pH of the mixture was 5 and the white precipitate obtained was filtered and discarded. The mother liquor was placed at room temperature on slow evaporation and after two weeks light pink single crystals suitable for X-ray determinations were obtained. Elemental analysis calculated for $ZnC_{46}H_{43}N_7O_{14}$ (982.4 g/mol): C, 56.2; H, 4.4; N, 10.0. Found: C, 56.4; H, 4.4; N, 10.2. The thermogravimetric analysis (Fig. S4) confirmed the presence of seven labile water molecules per zinc atom (weight loss: Exp.: 12.4% Calc.: 12.8%; broad endothermic peak, DTA, 57 °C). The weight loss (91.7%, calc.; 91.3%, exp.) at 800 °C and represents the formation of ZnO (characterized by FTIR spectroscopy).

2.3. X-ray diffraction data

The measurements were performed on an Oxford Xcalibur Gemini, Eos CCD diffractometer with graphite-monochromated MoKα (λ = 0.71073 Å) radiation. X-ray diffraction intensities were collected (ω scans with ϑ and κ-offsets), integrated and scaled with CrysAlisPro [12] suite of programs. The unit cell parameters were obtained by least-squares refinement (based on the angular settings for all collected reflections with intensities larger than seven times the standard deviation of measurement errors) using CrysAlisPro. Data were corrected empirically for absorption employing the multi-scan method implemented in CrysAlisPro. The structure was solved by intrinsic phasing with SHELXT of the SHELX suit of programs [13] and the corresponding molecular models developed by alternated cycles of Fourier methods and full-matrix least-squares refinement with SHELXL of the same package. The molecular model showed disordered NO_3^- anion and water molecules, whose contribution to the diffraction pattern was removed from the data set with the procedure described by Van der Sluis and Spek [14] and implemented in the program SQUEEZE included in PLATON [15] suit of programs. As

expected the refinement improved substantially to a degree where all H-atoms of the remained ordered $[Zn(phen)_3](CCA)$ portion of the molecular structure were found among the first 31 residual peaks of a difference Fourier map phased on the heavier atoms. These light atoms, however, were positioned on stereo-chemical basis and refined with the riding model.

Table 1. Crystal data and structure refinement results for $[Zn(phen)_3](CCA)(NO_3).xH_2O$.

Empirical formula	$C_{46}H_{29}N_7O_7Zn$	
Formula weight	857.13	
Temperature	297(2) K	
Wavelength	0.71073 Å	
Crystal system	Triclinic	
Space group	$P\bar{1}$	
Unit cell dimensions	a = 12.3818(5) Å	α = 113.768(3)°
	b = 15.1143(4) Å	β = 112.826(4)°
	c = 15.4875(6) Å	γ = 90.329(3)°
Volume	2399.25(17) $Å^3$	
Z	2	
Density (calculated)	1.186 Mg/m^3	
Absorption coefficient	0.564 mm^{-1}	
F(000)	880	
Crystal size	0.282 x 0.218 x 0.135 mm^3	
ϑ-range for data collection	3.206 to 29.449°	
Index ranges	$-16 \le h \le 16$, $-18 \le k \le 18$, $-18 \le l \le 21$	
Reflections collected	21439	
Independent reflections	10998 [R(int) = 0.036]	
Observed reflections	7408	
Completeness to ϑ = 25.242°	99.8 %	
Refinement method	Full-matrix least-squares on F^2	
Data / restraints / parameters	10998 / 0 / 514	
Goodness-of-fit on F^2	1.015	
Final R indices [I>2sigma(I)]	R1 = 0.0572, wR2 = 0.1629	
R indices (all data)	R1 = 0.0878, wR2 = 0.1836	
Largest diff. peak and hole	0.415 and -0.375 $e.Å^{-3}$	

[a] $R_1=\Sigma||F_o|-|F_c||/\Sigma|F_o|$, $wR_2=[\Sigma w(|F_o|^2-|F_c|^2)^2/\Sigma w(|F_o|^2)^2]^{1/2}$

Crystal data, data collection procedure, structure determination methods and refinement results are summarized in Table 1. Crystallographic structural data have been deposited at the Cambridge Crystallographic Data Centre (CCDC). Any request to the CCDC for this material should quote the full literature citation and the reference number CCDC 1587820.

2.4. Alkaline phosphatase specific activity

The effect of zinc(II), HCCA, phen and the binary and ternary complexes on ALP activity was determined by UV-Vis spectroscopy. The reaction was started by the addition of the substrate para-nitrophenyl phosphate (p-NPP) and the product p-nitrophenol was monitored by changes in the absorbance at 405 nm. Briefly, the experimental conditions for ALP specific activity measurement were as follows: 1 µg/mL of bovine intestinal ALP and 5 mM of p-NPP were dissolved in the incubation buffer (55 mM glycine + 0.55 mM $MgCl_2$, pH 10.4) and held for 10 min at 25 ºC. The effects of the compounds were determined by addition of different concentrations (1-100 µM) of each compound to the pre-incubated mixture. The solutions of the complexes were prepared in DMSO before adding them the buffer to obtain the desired final concentrations and the final concentration of DMSO in each tube did not exceed 1%. The effect of each concentration was tested at least in triplicate in three different experiments.

2.5. Antimicrobial assays

The antimicrobial activity was evaluated by the Minimum Inhibitory Concentration (MIC) using the agar dilution method. The grow/assay medium for all strains was Müeller-Hinton broth or agar [16,17]. The inocula of bacterial strains were prepared from 18 h-old broth cultures. A McFarland standard 0.5 suspension was prepared for each microorganism and a 1:10 dilution was made prior to inoculation (~10^7 colony forming units (CFU) per milliliter) [18,19]. The inocula of fungal strains were adjusted to 0.5 McFarland standard and the suspensions (~10^8

CFU per milliliter) were directly inoculated without dilution. For the agar dilution method, aqueous solutions of the metal salt ($Zn(NO_3)_2.6H_2O$) and the ligand phen were prepared and sterilized by filtration. The ligand HCCA and the zinc(II) complexes ZnCCA and ZnCCAphen were dissolved in DMSO and sterilized by filtration. Besides, two-fold serial dilutions were prepared from the stock solution into molten Mueller Hinton agar medium and cooled down to 45 °C to obtain the desired final concentrations. For each compound, the dosage started from 1.5 μg mL^{-1} and continued until 1500 μg mL^{-1} (stopping criteria). Then, the inoculum of 2 μL of the microbial suspensions was streaked onto the plates and incubated aerobically at 37 °C for 24 h (bacteria) and 48 h (fungi). Inhibition of microbial growth in the plates containing tested solutions was judged by comparison with growth in blank control plates. The MIC was defined as the lowest dilution of the compound that inhibited the visible growth of the tested organism.

3. Results and Discussion

3.1. Crystallographic structural results of {[Zn(phen)$_3$]CCA}$^+$

Figure 1 is an ORTEP [20] drawing showing the crystal packing of the salt ordered [Zn(phen)$_3$]CCA part. The ligand CCA appears in the lattice deprotonated at its carboxylic group, namely as 2-Oxo-2*H*-1-benzopyran-3-carboxylate (CCA) as a counterion. Because of the extended molecular orbital π-delocalization, the fused rings of CCA are planar [*rms* deviation of atoms from the best least-square plane of 0.0197 Å]. The carboxylate group departs slightly from the plane [angled at 30.8(6)º]. Bond distances and angles within the CCA anion accord with reported values in other coumarin salts [21–23], only differing with these salts in the dihedral angle subtended by the –COO group with the fused ring plane. As expected, the main differences in bond distances of CCA when compared with neutral coumarin-3-carboxylic acid [24] occurs due to the bond structure change at the carboxylic group upon deprotonation from formally C=O double and C-OH single bonds [lengths of 1.214 and 1.330 Å] in neutral HCCA to

two localized C-O σ-bond plus a delocalized π-bond in the –COO- carboxylate group of CCA (C-O bond distances of 1.245(4) and 1.268(5) Å).

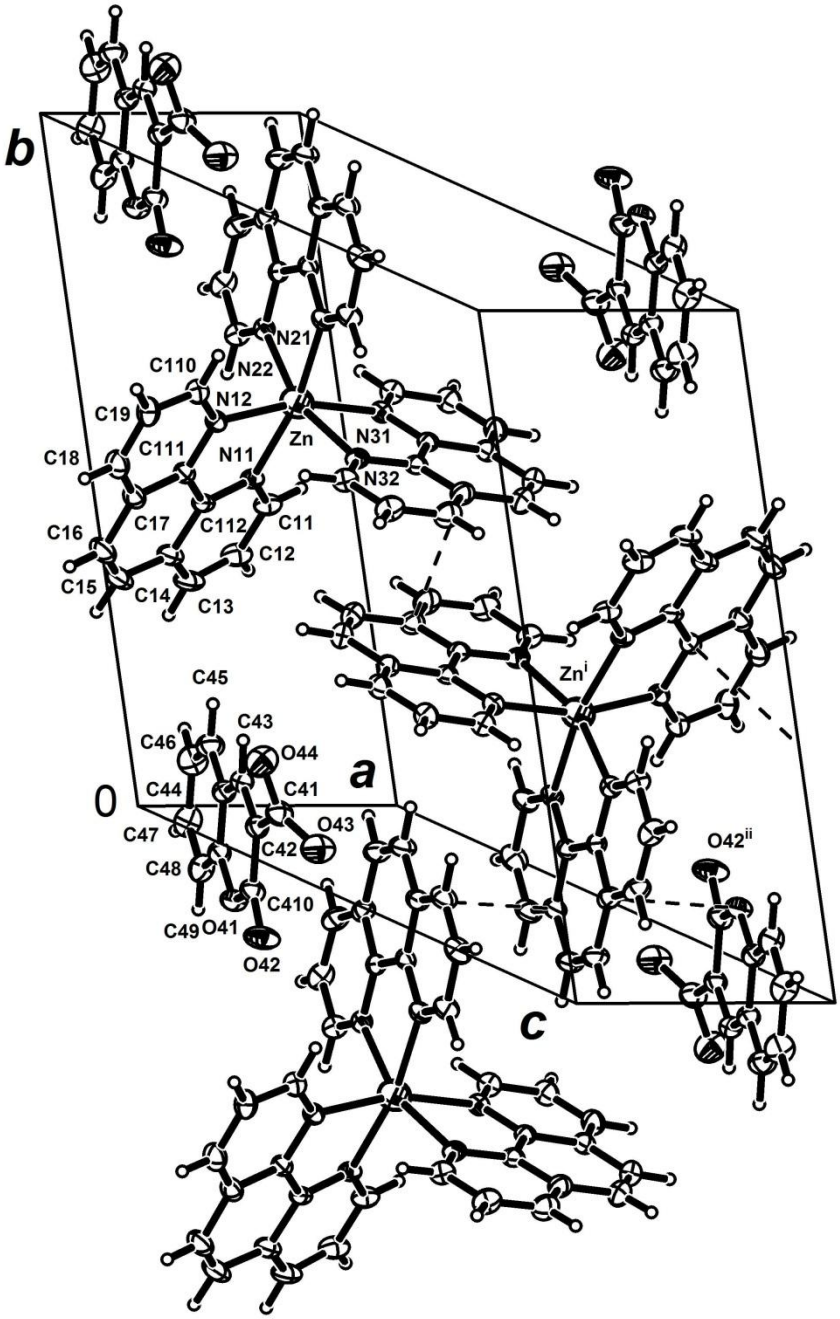

Fig. 1. Crystal packing of $\{[Zn(phen)_3](CCA)\}^+$ cation in $[Zn(phen)_3]CCA(NO_3).7H_2O$ solid showing the labeling of the non-H atoms and their displacement ellipsoids at the 30% probability level. For clarity, only one phenanthroline ligand was completely labeled to indicate the atom numbering scheme. Dashed lines indicate possible path for inter ring π-π interactions. The displayed molecules belong to the same lamella of the layered arrangement adopted by the $\{[Zn(phen)_3](CCA)\}^+$ cations. Crystal symmetry operations: (i) 1-x, 1-y, 1-z; (ii) 1-x, -y, 1-z.

Zinc ion in the $[Zn(phen)_3]^{2+}$ complex is located in a distorted octahedral environment (ZnN_6 core), coordinated to three phen groups acting as bidentate ligands through their N-atoms in a three-bladed propeller-líke conformation. Data of the crystal structure of the cation complex is in accordance with a previous report [25]. Briefly, metal-nitrogen bond distances are in the range from 2.138(2) to 2.199(2) Å. Phenanthroline N-Zn-N 'bite' angles are 77.17(9), 74.49(9) and 76.65(9)º; the other *cis* N-Zn-N angles are in the 89.94(9)-101.03(9)º range. *Trans* N-Zn-N bond angles range from 161.14(9) to 169.76(9)º.

The $\{[Zn(phen)_3]^{2+}$ and CCA^- ions are arranged in $\{[Zn(phen)_3](CCA)\}^+$ layers parallel to the crystal $(10\bar{1})$ plane (*cf*. Figure 1) which are further stabilized through π-π staking interaction between neighboring, symmetry-related, phenanthroline ligands (inter-fused ring distances in the range from 3.47 to 3.57 Å) and between phenanthroline and CCA rings (3.38 Å apart). The layers, in turn, are interspaced by nitrate anions (not shown) which are disordered around crystallographic inversion centers and by loosely bound and also disordered interstitial water molecules, as confirmed by the relatively low dehydration temperatures observed in DTA-DTG measurements.

3.2. Vibrational spectroscopy

The vibrational FTIR and Raman spectra of the three complexes, $[Zn(phen)_3]CCA(NO_3).7H_2O$, $[Zn(CCA)_2phen].4H_2O$ and $[Zn(CCA)_2(H_2O)_2]$ have been measured and compared with the spectra of phen, CCA and HCCA (Figs. 2 and 3). As it was previously mentioned, deprotonated CCA was found to act using two different types of interactions, as a counter anion in $[Zn(phen)_3]CCA(NO_3)$ or in a bidentate coordinated form in $[Zn(CCA)_2(H_2O)_2]$. Spectral comparison substantiated similarities between pairs of compounds. The FTIR pattern of ionic carboxylate in the KCCA salt resulted similar to the vibrational modes of CCA in the $[Zn(phen)_3]CCA(NO_3)$ complex showing that CCA is acting as counterion. Whereas, the bands corresponding to the modes of the carboxylate group assigned to CCA in $[Zn(CCA)_2phen].4H_2O$ are located near those of ZnCCA, showing a similar coordination mode of this group. Considering that the crystal structure of ZnCCA showed that the carboxylate group acted as a monodentate ligand and that chelation with CCA was achieved by C=O (carbonyl) coordination, we assume a similar environment of the metal ion in the ternary complex. Main vibrational modes of these compounds and the free ligands with their tentative assignments for FTIR and Raman spectra are listed in Table 2.

In the region between 3500 cm^{-1} and 2900 cm^{-1} broad and intense bands corresponding to O-H stretching modes can be found. For the zinc complexes, the bands can be assigned to coordinated water molecules (3221 cm^{-1} in ZnCCA) or hydration water (3336 cm^{-1} for ternary complex and 3389 cm^{-1} for the binary Znphen complex). For HCCA, and due to presence of an intramolecular H-bond, the band shifts to lower frequencies and it is located at 2933 cm^{-1}.

Considering the polarization produced by the interactions in the different compounds, the carbonyl ν(C=O) stretching modes shifted to lower values due to the elongation of C=O bond upon hydrogen bonding or coordination to the metal center (Table 3). In HCCA the C=O (carbonyl) group is involved in an intramolecular H-bond by formation of a 5-membered ring, and according to its crystalline structure [26], its bond length is 1.216 Å and then, the frequency

assigned to the C=O stretching mode is 1682 cm^{-1}. After deprotonation, the ionic CCA decreases the polarization of the C=O moiety and the bond is shortened to 1.199 Å, for $[Zn(phen)_3](CCA)(NO_3)$, therefore, the frequency is shifted to 1733 cm^{-1}. On the other hand, when CCA is acting as a bidentate ligand (though two O atoms belonging to carboxylate and carbonyl moieties) in ZnCCA, the formation of a 5-membered ring produces an elongation of the C=O length (1.232 Å) and its frequency shifted to the red (1669 cm^{-1}). These results are in agreement with the experimental results obtained by B.S. Creaven et al. for the powder complex of ZnCCA [3], but the structure proposed by these authors is different from the structure determined by X-ray measurements. The position of the C=O (carbonyl) stretching band in ZnCCAphen at 1670 cm^{-1} is an indication of the coordination of the carbonyl group to the metal center like in the binary complex.

The C=O stretching band of the carboxylic acid of HCCA appeared as a strong band at 1744 cm^{-1} (FTIR) and as a medium band 1738 cm^{-1} (Raman) in agreement to the measured C=O bond length of 1.199 Å [26]. Upon deprotonation this band disappeared and two new bands corresponding to the symmetric and antisymmetric CO stretching of the carboxylate groups are observed (see Table 3) [27]. These bands have been assigned by comparison with previously reported data [23,28]. Besides, the band corresponding to the symmetric (COO^-) stretching showed higher intensity in the Raman spectra, as expected. The CO bond lengths for the monodentate and anionic carboxylate group obtained in this work agree with those reported for similar complexes with Cu(II), Mn(II), Cd(II) and Zn(II) metal centers (Table 4). Metal coordination to the C=O (carbonyl) group generates the same effect than H-bonds (-C=O…H) in the ligand, due to the delocalization of the π electrons that reduces the electron density of the C=O bond which weakens and elongates it, generating partial double bond character. It is evident that in anionic CCA the C=O group lacks of resonance and hence it remains double bonded (C=O, 1.199 Å). Both the C=O lengths for the carboxylic acid and carbonyl groups are identical (Tables 3 and 4) and then, the stretching frequencies C=O (carboxylic) for HCCA and

C=O (carbonylic) for Znphen appeared in the same region of the infrared spectrum (1738 cm^{-1}, Raman, Table 2) [29]. It can then be seen that the distance changes in HCCA upon deprotonation for the C=O group of carboxylic acid (from 1.199 Å to ca. 1.25 Å) and for the C=O carbonylic group (carbonyl with H-Bridge interaction, 1.216 Å to double bonded carbonyl, 1.199 Å) (Table 3) was found to be a controversial factor that produced misinterpretations in the FTIR spectra of complexes containing coumarin-3-carboxylic acid.

The spectral region most characteristic of any given phen-metal complex is the 900-700 cm^{-1} spectral range. The characteristic and most intense phen bands are located at 853 cm^{-1} and 738 cm^{-1}. These bands have been assigned to motions of ring hydrogen atoms moving in phase out of the plane of the ring. The high energy band has been identified to the out of plane motion of the hydrogen atoms on the center ring and the band at 738 cm^{-1}, to the hydrogens on the heterocyclic rings [30]. The shift of these bands appeared sensitive to small differences in the nature of the coordinated metal ion [31]. Hence, the small shifts of these bands at 850 cm^{-1} and 729 cm^{-1} in the ternary complex and at 847 cm^{-1} and 730 cm^{-1} in the $[Zn(phen)_3]^{+2}$ salt, are indicative of the phen coordination to the metal center. Other vibrational modes of phenanthroline ligand appeared as low intense bands in the FTIR spectra of the metal complexes. The region of characteristic ring frequencies of aromatic compounds is located in the 1600-1400 cm^{-1} range and the vibrational modes of phen ligands of medium intensities and associated with C=C and C=N stretchings overlapped with those of CCA [31]. The low intensity C=C and C=N stretching bands at *ca.* 1620 and 1646 cm^{-1}, respectively, are masked with the C=C and C=O stretching modes of the CCA ligand.

Besides, the sharp band at 1384 cm^{-1} for $[Zn(phen)_3](CCA)(NO_3)$ has been assigned to stretching mode of nitrate anion acting as counterion like CCA [27].

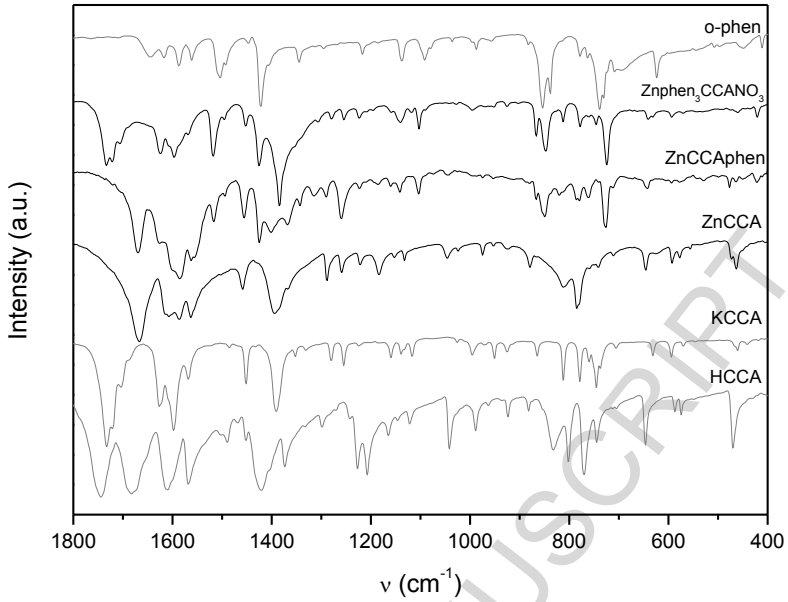

Fig. 2. FTIR spectra of o-phenanthroline dihydrate (phen), $[Zn(phen)_3]CCA(NO_3)$ ($Znphen_3CCANO_3$), $[Zn(CCA)_2phen].4H_2O$ (ZnCCAphen), $[Zn(CCA)_2(H_2O)_2]$ (ZnCCA), coumarin-3-carboxylate potassium salt (KCCA) and coumarin-3-carboxylic acid (HCCA).

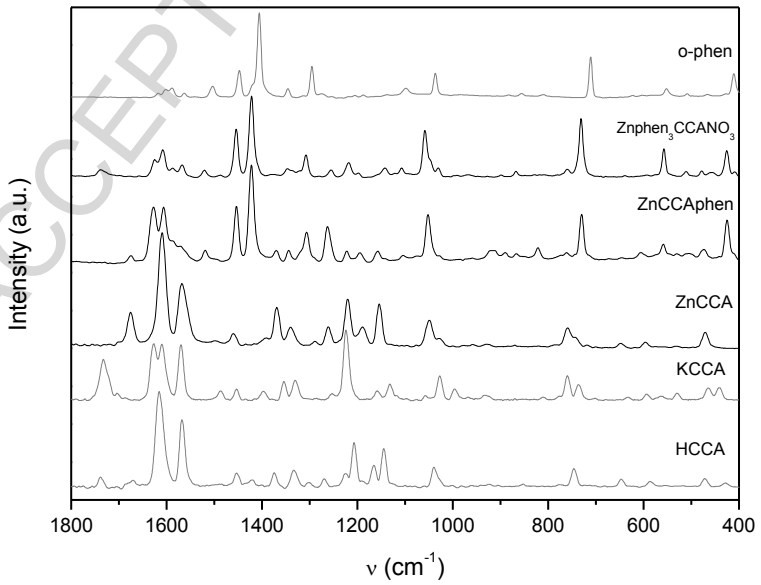

Fig. 3. Raman spectra of o-phenanthroline dihydrate (phen), $[Zn(phen)_3]CCA(NO_3)$ ($Znphen_3CCANO_3$), $[Zn(CCA)_2phen].4H_2O$ (ZnCCAphen), $[Zn(CCA)_2(H_2O)_2]$ (ZnCCA), coumarin-3-carboxylate potassium salt (KCCA) and coumarin-3-carboxylic acid (HCCA).

Table 2. Main vibrational modes observed by FTIR and Raman (bold) of different compounds with Zn(II), HCCA and phen (dihydrate).

Assignment	**HCCA**	**KCCA**	**ZnCCA**	**phen**	**ZnCCAphen**	**Znphen**
ν OH (H_2O)			3221 (br)	3408 (br)	3336 (br) 3261 (br)	3389 (br)
ν OH (bridge)	2933 (s)					
ν C=O (carboxylic)	1744 (s) **1738 (m)**					
ν C=O (carbonyl)	1682 (s) **1680 (w)**		1669 (s) **1675 (m)**		1670 (s) **1675 (w)**	1733 (s) **1738 (m)**
ν C=C	1609 (s) **1615 (s)**	1627 (s) **1627 (s)**	1616 (s)		1625 (s) **1627 (s)**	1624 (s) **1625 (s)**
		1608 (sh) **1609 (s)**	1609 (m) **1609 (s)**		1598 (sh) **1606 (s)**	1607 (sh) **1608 (s)**
ν_{as} COO		1597 (s) **1599 (sh)**	1563 (m) **1567 (m)**		1563 (s) 1555 (s) **1560 (w)**	1596 (m) **1589 (m)**
ν_s COO		1391 (sh) **1396 (m)**	1367 (w) **1369 (m)**		1367 (m) **1369 (m)**	
ν_s COO + ν_3 NO_3						1384 vs, br **1422 vs (phen)** **1377 w**
ν_1 NO_3						**1057 s**
phen				853 (s) **855 (w)**	850 (s)	847 (s)
phen				738 (s)	725 (s) **729 (s)**	724 (s) **723 (sh)**

Abbreviations: vs, very strong; s, strong; m, medium; w, weak; sh, shoulder; br, broad. ν, stretching; s, symmetric; as, antisymmetric.

Table 3. Comparison of bond lengths and vibrational stretchings for CO (carbonyl, carboxylic acid and carboxylate) groups.

	HCCA [a]		**ZnCCA** [b]		**Znphen**	
	Bond length (Å)	ν C=O (cm^{-1})	Bond length (Å)	ν C=O (cm^{-1})	Bond length (Å)	ν C=O (cm^{-1})
C=O (carboxylic)	1.199	1744 (s)				
CO (carboxylate)			1.245 1.264	1561 1396	1.245 1.268	1596 1384
C=O (carbonyl)	1.216	1682 (s)	1.232	1669 (s)	1.199	1733 (s)

[a] Crystallographic data for HCCA obtained from [26]; [b] Crystallographic data measured in this work for comparison with data obtained by Y. Cui et al. [10].

Table 4. Comparison of CO bond lengths for the carbonyl, carboxylic and carboxylate groups.

	HCCA [26]	CuCCA [32]	MnCCA [33]	CdCCA [34]	ZnCCA [b]	ZnCCA[a]	CCA[a] anion
C=O carbonyl	1.216	1.216	1.222	1.227	1.2241	1.232	1.199
C=O carbox	1.199	1.251 1.266	1.2509 1.2549	1.256 1.257	1.2501 1.2617	1.245 1.264	1.245 1.268
C-O(H) carbox	1.328						

[a] Comparison of crystallographic data measured in this work and [b] data obtained by Y. Cui et al. [10].

3.3. NMR spectroscopy

The ^{1}HNMR, ^{13}CNMR and ^{1}H-^{13}C HSQC spectra have been measured in DMSO-d_6, and the proposed assignments were carried out using standard 2D correlation techniques Table 5 and Figs. S5-S8. Assignments for HCCA spectrum are in agreement with previous reports [35], similar to the assignment of the complexes [3,5]. Fig. 4 shows the carbon atom numbering.

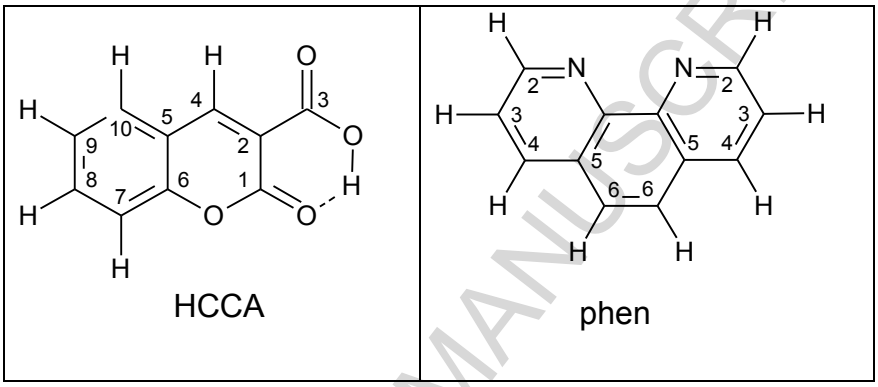

Fig. 4. Carbon atom numbering for HCCA and phenanthroline.

The broad signal at 13.25 ppm in the ^{1}HNMR spectrum of HCCA has been assigned to the acid proton of the carboxylic group which is involved in an intramolecular H bond. When this H atom is dissociated, this signal disappears (KCCA and the Zn complexes). The negative charge in CCA is delocalized all over the molecule and, as a consequence, an increment in the shielding of every proton is observed and every signal shifts to upper fields. The major shift has been obtained for the H(4) signal because of its proximity with the carboxylate group. The HCCA peak at 8.76 ppm shifts 0.94 ppm in the ionic compound (7.82 ppm) while in the complexes the shifts are 0.23 ppm and 0.61 ppm for ZnCCA and ZnCCAphen, respectively.

The ^{1}H chemical shifts for the phen molecule with four pairs of equivalent protons, can be ordered: H(2) > H(4) > H(6) > H(3) [36], in which the lowest field peak can be assigned to the

nitrogen-adjacent proton, H(2). It has been reported that after complexation all the signals are both shifted downfield and broadened [37] and that the most pronounced changes upon the formation of the Zn(II) phenanthroline complexes are observed for the phen fragment and for protons at C(2) which indicates the engagement of aromatic nitrogen atoms in the binding of the metal ion [38]. However, some authors propose a change in this order, mainly due to a significant shielding in H(2). [39] Although we have observed this magnitude of shielding (from 9.18 ppm in free phen [36] to 8.78 ppm in the ternary complex), we propose similar order to that of free-phen based mainly on the ZnCCAphen HSQC spectrum. In this spectrum, the highest downfield shifts for ^{13}C have been assigned to the C(4) atom of CCA (carboxylic-adjacent carbon) and the C(2) atom of phen (nitrogen-adjacent carbon). As a consequence, in the ternary complex, we have assigned the δ value of 8.15,143 ppm (^{1}H,^{13}C) to H,C(4) of CCA and 8.78,139 ppm to H(2) of phen (Fig. 5).

From the 2D HSQC spectra of the complexes (Fig. 4) it can be observed that the signals of coupling ^{1}H-^{13}C for the ZnCCA complex shift to a shielded position (up and right) in comparison with the ZnCCAphen complex. In addition, four additional signals assigned to phen appear in the ternary complex. Hence, we propose that the coordination of an electron donor base such as phen to ZnCCA, causes a shielding increase and downfield shifts of all protons of CCA in the ternary complex.

Besides, for the carbonyl carbon atom, C(1), the ^{13}C δ signal also shows significant shifts. In HCCA the lactone carbonylic group is involved in intramolecular H- bridge with a δ ^{13}C value of 157 ppm. Once deprotonated, δ ^{13}C shifted to 153 ppm. In the coordination complexes, a 5-membered rings are formed between zinc(II), and the carboxylic and carbonylic groups. Therefore, the measured values for δ ^{13}C are closer to that of HCCA rather than that of KCCA, as expected.

With the aim to establish the coordination mode of the carboxylate group we compared the measured δ ^{13}C values for C(3). In the acid HCCA, δ ^{13}C was located at 164 ppm and shifted downfield as expected, to 165 ppm in the potassium salt (δ salt < δ acid) [40]. When the carboxylate group coordinates to the metal ion the δ ^{13}C value of was located at 167 ppm for both, the binary and the ternary complexes. Although it was predicted that coordination may lead to lower ^{13}C chemical shifts in comparison with ionic compounds [40], we have found a deshielding of this carbon atom, similar to other metal complexes of CCA [5,41]. Hence, the HSQC spectra measured for CCA allow us to solve the reported inconsistencies [3,35]. This behavior has been explained on the basis of the inductive effects that can affect the entire molecule for highly conjugated compounds [42,43].

By FTIR spectroscopy the monodentate coordination mode of the carboxylate anion was determined (see above). In both complexes, the measured chemical shifts for C(3) were 167 ppm, showing a similar mode of coordination to the metal. However, the coordination mode could not be predicted by these spectral measurements because there were no differences between these chemical shifts.

Table 5: ^{1}H and ^{13}C NMR main chemical shifts in DMSO-d_6 of HCCA, KCCA and binary and ternary complexes of Zn(II).

	Group	HCCA		KCCA		ZnCCA		ZnCCAphen		phen [38]	
		^{1}H	^{13}C	^{1}H	^{13}C	^{1}H	^{13}C	^{1}H	^{13}C	^{1}H	^{13}C
CCA	**C(3)OOH**	13.25 (s)	164	-	165	-	167	-	167		
	C(1)=O	-	157	-	153	-	158	-	158		
	CH (4)	8.76 (s)	149	7.82 (s)	137	8.53 (s)	145	8.15 (s)	143		
	CH (7)	7.92 (d)	130	7.67 (d)	128	7.85 (d)	130	7.64 (d)	129		
	CH(10)	7.74 (t)	135	7.50 (t)	130	7.65 (t)	133	7.57 (t)	133		
	CH(8)	7.44 (m)	116	7.29 (m)	116	7.39 (m)	116	7.28 (m)	116		
	CH(9)	7.42 (m)	125	7.27 (m)	124	7.36 (m)	125	7.27 (m)	125		
phen	**CH(2)**	-		-		-		8.78 (br)	139	9.18	150.4
	CH(3)	-		-		-		7.25 (br)	129	7.62	123.1
	CH(4)	-		-		-		8.18 (br)	127	8.23	136.0
	CH(6)	-		-		-		7.93 (br)	125	7.77	126.6

Chemical shifts are expressed in ppm using TMS as reference. In parentheses the signal multiplicities are indicated (s: singlet, d: doublet, t: triplet, m: multiplet, br: broad).

Fig. 5: 2D ^{1}H,^{13}C HSQC NMR spectra overlapping of binary ZnCCA and ternary ZnCCAphen complexes

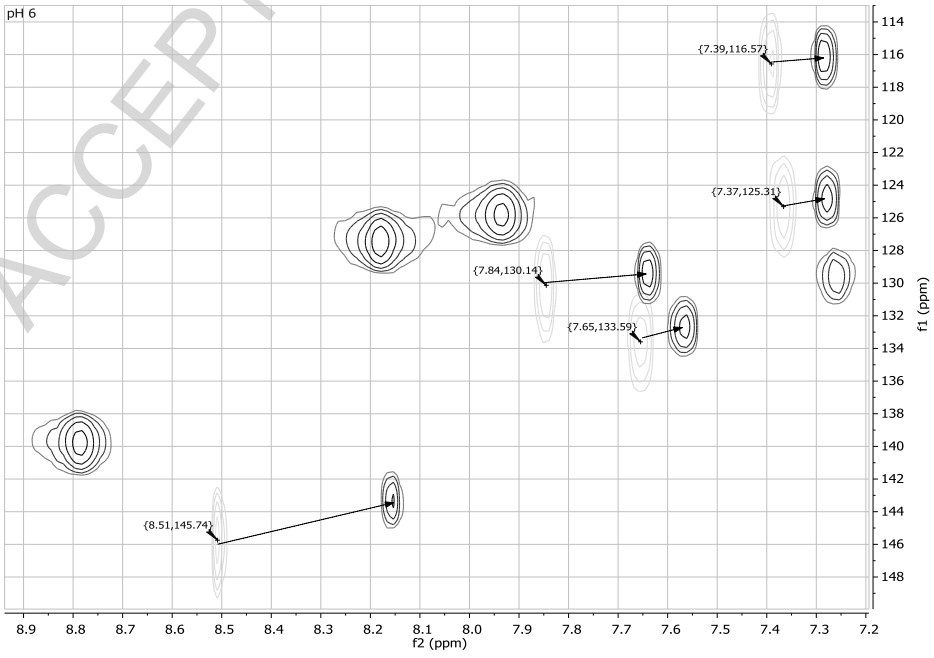

3.4. Alkaline Phosphatase

Alkaline phosphatase (ALP) is one of the most important zinc-dependent enzymes. It has been reported that Zn(II) increases the ALP activity at low concentrations [44], nevertheless, in higher concentrations the metal can displace the Mg(II) ion from the active site, preventing its stabilizing effects [45]. ALP can be found in almost every tissue of the body, mainly in the liver and in the bones. It is also a hydrolase enzyme responsible for removing phosphate groups from several types of molecules such as nucleotides, proteins, and alkaloids. As it is suggested by its name, alkaline phosphatases are more effective in an alkaline environment. ALP activity in serum is usually related to bone and liver diseases *in-vivo* and it is a marker of osteoblastic differentiation [46]. Furthermore, the chelating ligand phen also produces inhibition of intestinal bovine ALP. This effect has been explained by a time-dependent mechanism in which Zn(II) is slowly removed from ALP, causing its inactivation. However, this effect has shown to be reversible, in contrast with the effect exerted by other chelating compound, EDTA [47,48].

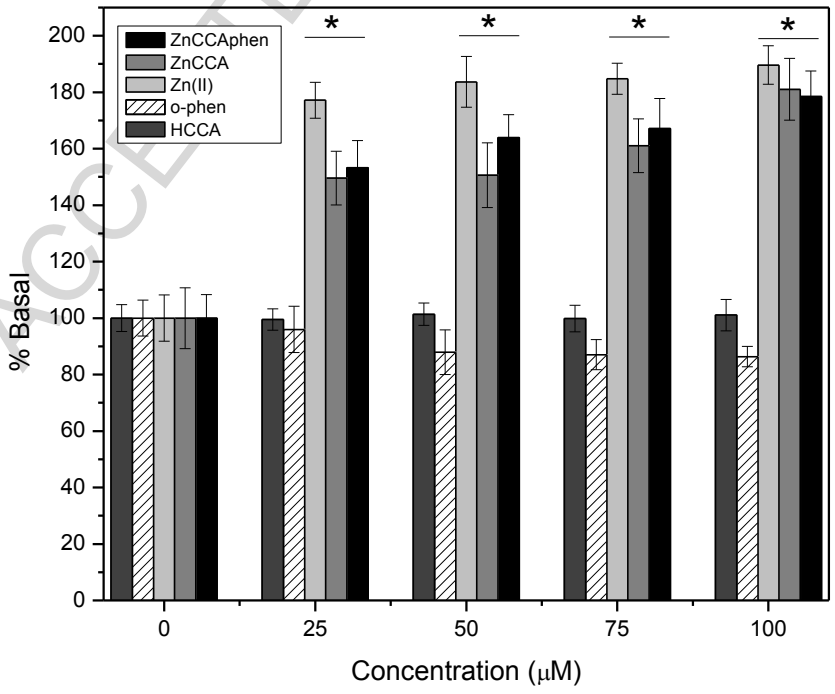

Fig. 6. The effects of the different compounds on ALP activity obtained from bovine intestinal mucose. Initial rate was determined by incubation of the enzyme at 37ºC for 20 min in the absence or presence of variable concentrations of each compound. The ALP basal activity was 5.2 ± 0.2 nmol pNPP min^{-1} μg^{-1} protein. The results are expressed as the percentage of the basal level and represent the mean ± SEM (n = 9). *Significant differences versus control $p < 0.05$.

Herein, we have tested the effect of the binary and ternary complexes in addition to HCCA, phen, and Zn(II) on ALP activity. In the tested range of concentrations, Zn(II) has increased the ALP activity in almost 90% from de basal conditions at a concentration of 100 μM (Fig. 6). According to what was aforementioned, low concentrations (less than 1 mM) of Zn(II) increase the enzyme reaction rate [44], and in consequence, its activity. Moreover, no significant differences among the two complexes and Zn(II) were found at 100 μM concentration. HCCA has not shown any difference in ALP activity in the tested concentrations (up to 100μM). In addition, phen has only shown a slightly inhibition (14%) at the maximum concentration tested. According to the chelating character of phen, ALP activity decreases due to complexation of Zn(II) from the active site [47]. This inhibition is relatively low at 100 μM, however it increases in a significant manner at 10 time higher concentrations, with an inhibition of ALP activity of 59 % at 1 mM [49].

To sum up, at the low tested concentrations it has been observed an increment in ALP activity for the complexes, like the effect of Zn(II). HCCA has not shown activity, while phen slightly decreases ALP activity. Due to the low solubility of complexes, concentrations higher than 100 μM could not be measured.

3.5. Microbiological assays

It has been reported that some coumarinic derivatives [49] and some metal complexes of HCCA have antimicrobial effects [2]. Hence, we propose to study the activity of the binary and ternary complexes, in addition to HCCA, phen, and Zn(II) for comparative purposes against different bacterial and fungal strains with clinical interest. The antimicrobial effect was evaluated by the minimum inhibitory concentration (MIC) technique, the lowest dilution of the compound that inhibited the visible growth of the tested organism. The effects of the compounds have been tested on five strains of bacteria derived from the American Type Culture Collections (ATCC), namely *Pseudomonas aeruginosa (P. aeruginosa,* ATCC 27853*)*, *Escherichia coli (E. coli), Enterococcus faecalis (E. faecalis,* ATCC 29212*)*, *Staphylococcus aureus (S. aureus,* ATCC 25923*)*, *Staphylococcus epidermidis (S. epidermis,* ATCC 1263*)*. The antifungal activity was tested on five strains of fungus, *Candida parapsilosis (C. parapsilosis,* ATCC 22019*)*, *Candida krusei (C. krusei*), *Candida glabrata (C. glabrate)*, *Candida albicans (C. albicans), Candida tropicalis (C. tropicalis)* these last obtained from clinical isolates. It is well-known that the antibacterial activity is significant when MIC values are 100 μg mL^{-1} or lower. MICs in the 100 a 500 μg mL^{-1} range are considered moderate, between 500 a 1000 μg mL^{-1} weak, and inactive above 1000 μg mL^{-1} [50,51].

The activities for Zn(II) and phen have previously been reported by our group [52]. The ligand phen has shown significant antimicrobial activity against both, fungi and bacteria in every tested strain (except in *P. aeruginosa*, MIC of 375 μg mL^{-1}). *P. aeruginosa*, is the only strain of aerobic bacteria tested, and has shown the lowest effect after each treatment with the different compounds. On the other hand, *E. coli* has shown not only to be sensitive to phen (MIC of 12 μg mL^{-1}) but also to Zn(II) (MIC of 188 μg mL^{-1}). This moderated value for the metal, in addition to significant activity against phen was also observed in both, *S. Aureus* and *S. epidermis*. Furthermore, these bacteria strains have shown to be slightly sensitive to the ternary complex

(Table 6). The binary complex of ZnCCA has not exhibited neither antifungal nor antibacterial activity. However, the ternary complex of ZnCCAphen has shown antifungal activity and a significant improvement of the antifungal activity of HCCA, ZnCCA and Zn(II) ions due to complexation with phen. The highest effect was observed in *C. albicans* in which phen has shown a MIC of 3 μg mL^{-1} and the ternary complex displayed a MIC of 12 μg mL^{-1}. Besides, it has been discarded that these activities could be due to free phen generated by a possible release of this ligand from the complex because of the different relative results obtained in the tested strains. It has been stated that phenanthrolines have potential biological activities such as anticancer, antiviral and antimicrobial agents and that their interaction with DNA occurs between base pairs by aromatic π stacking [53]. The higher antimicrobial effects of the ternary complex in comparison with the lack of antimicrobial activity of ZnCCA, allow us to postulate that the phen ligand gave the planar structure in the complex needed for the cleavage of the DNA of the different strains being this effect higher for the Candida strains. The higher antifungal activity for phenanthroline coordinated to metal centers has previously been shown [54,55]. The MIC values of ZnCCAphen differ slightly from the values determined for the antibacterial effects of other ternary complex of Zn(II) with 4-methylpiperazine-1-carbodithioate and phenanthroline against *E.coli, P aeruginosa, S. aureus and E. faecalis* that are in the range of 128-256 μg mL^{-1} [56]. Interestingly, for the Zn complex of phenanthroline and bipyridine, $[Zn(bipy)_2(phen)]Cl_2.6H_2O$, in which both ligands could display π stacking, the antifungal MIC values are somehow lower than in ZnCCAphen and ranged from 4.88 μg mL^{-1} for *C. albicans,* 9.76 μg mL^{-1} for *C.Krusei* and 39 μg mL^{-1} for *C. Parapsilosis* [57].

To sum up, HCCA has not shown antimicrobial activity in any of the tested strains, in agreement with previous reports [5]. A similar behavior has been observed for ZnCCA. Moreover, Zn(II) has shown none to mild (in *E. coli, S aureus* and *S. epidermis*) antimicrobial effects at the low concentration tested, in agreement with its essentiality for all living organisms. Although it has been widely demonstrated that phen is an antimicrobial compound [56], we have observed a

lower effect in bacterial (prokaryotic) than in fungal strains (eukaryotic), (the highest effect were in *C. albicans, C. glabrata* y *C. krusei)*. A similar behavior was observed for the ternary complexes.

It has been suggested that microbial infections are very common in hepatic diseases and there also exists a relationship between alkaline phosphatase and fungal and bacterial infections. Particularly, when those infections are present, ALP levels decreases [58]. Although we have found an increase in ALP activity for the tested complexes, we cannot establish a correlation with the antimicrobial activity. While the ALP activity seems to be related to Zn(II) presence, the antimicrobial activity seems to be related to the coordination of phen in the complexes.

Table 6. Minimum inhibitory concentration (MIC) of metal Zn(II), free ligands (phen and HCCA), binary complex ZnCCA and ternary complex ZnCCAphen for fungus and bacteria reference strains, in μg mL^{-1}. Minimum inhibitory concentration (MIC, μg mL^{-1}): Inactive (above 1000), weak toxicity (1000-500), moderate (500-100), significant toxicity (lower than 100). Minimum values are shown in bold.

		Zn(II)	phen	HCCA	ZnCCA	ZnCCAphen
Bacteria	*P. aeruginosa*	1500	375	1500	>1500	>1500
	E. faecalis	1500	**94**	1500	>1500	1500
	E. coli	188	**12**	>1500	>1500	1500
	S. aureus	188	**24**	1500	>1500	750
	S. epidermidis	188	**12**	1500	1500	750
Fungi	*C. albicans* ATCC 10231	1500	**3**	>1500	>1500	**12**
	C. glabrata	1500	**6**	>1500	>1500	**24**
	C. krusei	1500	**6**	>1500	>1500	**24**
	C. parapsilosis ATCC 22019	750	**12**	>1500	>1500	**188**
	C. tropicalis	750	**12**	>1500	>1500	**188**

4. Conclusions

Coordination complexes containing Zn, coumarin-3-carboxylate and phen were obtained and characterized in solid state as well as in solution phase by elemental analysis, thermogravimetric studies, FTIR, Raman and NMR spectroscopies. The binary complex ZnCCA was prepared by previously reported procedures and characterized to make relevant comparisons. The reported structural data of ZnCCA (compared with our own determinations) and the determination of the structure of the new $[Zn(phen)_3](CCA)(NO_3)$ complex allowed us to complete the vibrational assignments considering that the CCA ligand in the latter complex is present as counteranion. Hence, vibrational determinations of the ternary complex ZnCCAphen have been performed by comparison with the binary complex. Some biological measurements were performed for both complexes coordinated to CCA, the ligands and the Zn(II) metal. The antimicrobial effects resulted relevant on the fungal studied strains. Because the complexes enhanced FAL activity they may eventually be useful to reverse the decrease of this activity when microbial infections were present.

Acknowledgments

This work was supported by CICPBA, UNLP (Project 11/X709, 11/X736), CONICET (PIP 0611, 0651 and 0651) and ANPCyT (PICT-13-0569, PME-06-2804 and PICT-06-2315) of Argentina. MSI and JJMM are fellowship holders from CONICET. EGF, GAE and OEP are research fellows of CONICET. PAMW is a research fellow of CICPBA, Argentina. MSI wants to thank Claudia Nuñez from Let´s Try for her writing assistance.

Supplementary Information Available. Tables of fractional coordinates and equivalent isotropic displacement parameters of the non-H atoms (Table S1), Full bond distances and

angles (table S2), atomic anisotropic displacement parameters (Table S3) and hydrogen atoms positions (Table S4). Figures of the thermal decomposition (TGA-DTA) of KCCA (Fig. S1), $[Zn(CCA)_2(H_2O)_2]$ (Fig. S2), $[Zn(CCA)_2phen].4H_2O$ (Fig. S3) and $[Zn(phen)_3](CCA)(NO_3).7H_2O$ (Fig. S4); Figures of 2D $^{1}H,^{13}C$ HSQC NMR spectrum of HCCA (Fig. S5), KCCA (Fig. S6), $[Zn(CCA)_2(H_2O)_2]$ (Fig. S7) and $[Zn(CCA)_2phen].4H_2O$ (Fig. S8). Full FTIR spectra 4000-400 cm^{-1} (Fig. S9)

References

[1] G. Borges Bubols, D. da Rocha Vianna, A. Medina-Remon, G. von Poser, R. Maria Lamuela-Raventos, V. Lucia Eifler-Lima, S. Cristina Garcia, The Antioxidant Activity of Coumarins and Flavonoids, Mini-Reviews Med. Chem. 13 (2013) 318–334. doi:10.2174/1389557511313030002.

[2] B. Thati, A. Noble, R. Rowan, B.S. Creaven, M. Walsh, M. McCann, D. Egan, K. Kavanagh, Mechanism of action of coumarin and silver(I)-coumarin complexes against the pathogenic yeast Candida albicans., Toxicol. In Vitro. 21 (2007) 801–8. doi:10.1016/j.tiv.2007.01.022.

[3] B.S. Creaven, M. Devereux, I. Georgieva, D. Karcz, M. McCann, N. Trendafilova, M. Walsh, Molecular structure and spectroscopic studies on novel complexes of coumarin-3-carboxylic acid with Ni(II), Co(II), Zn(II) and Mn(II) ions based on density functional theory., Spectrochim. Acta. A. Mol. Biomol. Spectrosc. 84 (2011) 275–85. doi:10.1016/j.saa.2011.09.041.

[4] I. Georgieva, T. Mihaylov, N. Trenda, N. Trendafilova, Lanthanide and transition metal complexes of bioactive coumarins: Molecular modeling and spectroscopic studies, J. Inorg. Biochem. 135 (2014) 100–112. doi:10.1016/j.jinorgbio.2014.03.003.

[5] B.S. Creaven, D. a. Egan, K. Kavanagh, M. McCann, A. Noble, B. Thati, M. Walsh, Synthesis, characterization and antimicrobial activity of a series of substituted coumarin-3-carboxylatosilver(I) complexes, Inorganica Chim. Acta. 359 (2006) 3976–3984. doi:10.1016/j.ica.2006.04.006.

[6] S. Chandraleka, K. Ramya, G. Chandramohan, D. Dhanasekaran, A. Priyadharshini, A. Panneerselvam, Antimicrobial mechanism of copper (II) 1,10-phenanthroline and 2,2′-bipyridyl complex on bacterial and fungal pathogens, J. Saudi Chem. Soc. 18 (2014) 953–962. doi:https://doi.org/10.1016/j.jscs.2011.11.020.

[7] J.E. Coleman, Zinc Proteins: Enzymes, Storage Proteins, Transcription Factors, and Replication Proteins, Annu. Rev. Biochem. 61 (1992) 897–946. doi:10.1146/annurev.bi.61.070192.004341.

[8] S. Tubek, P. Grzanka, I. Tubek, Role of zinc in hemostasis: a review., Biol. Trace Elem. Res. 121 (2008) 1–8. doi:10.1007/s12011-007-8038-y.

[9] P.M. May, P.W. Linder, D.R. Williams, Computer simulation of metal-ion equilibria in biofluids: models for the low-molecular-weight complex distribution of calcium(II), magnesium(II), manganese(II), iron(III), copper(II), zinc(II), and lead(II) ions in human blood plasma, J. Chem.

Soc. Dalt. Trans. (1977) 588–595. doi:10.1039/DT9770000588.

[10] Y. Cui, Q. Gao, H.-H. Wang, L. Wang, Y.-B. Xie, Diaquabis(2-oxo-2 H -chromene-3-carboxylato)zinc(II), Acta Crystallogr. Sect. E Struct. Reports Online. 67 (2011) m69–m69. doi:10.1107/S1600536810050865.

[11] I. Georgieva, N. Trendafilova, B.S. Creaven, M. Walsh, A. Noble, M. McCann, Is the CO frequency shift a reliable indicator of coumarin binding to metal ions through the carbonyl oxygen?, Chem. Phys. 365 (2009) 69–79. doi:10.1016/j.chemphys.2009.10.004.

[12] Oxford Diffraction Ltd., CrysAlisPro, version 1.171.33.48 (release 15-09-2009), (2009). CrysAlis171.NET.

[13] G.M. Sheldrick, A short history of SHELX, Acta Crystallogr. Sect. A. 64 (2008) 112–122. doi:10.1107/S0108767307043930.

[14] P. Van der Sluis, A.L. Spek, BYPASS: an effective method for the refinement of crystal structures containing disordered solvent regions, Acta Crystallogr. Sect. A. 46 (1990) 194–201. doi:10.1107/S0108767389011189.

[15] A.L. Spek, PLATON, A Multipurpose Crystallographic Tool, (1998).

[16] A. Klancnik, S. Piskernik, B. Jersek, S.S. Mozina, Evaluation of diffusion and dilution methods to determine the antibacterial activity of plant extracts., J. Microbiol. Methods. 81 (2010) 121–6. doi:10.1016/j.mimet.2010.02.004.

[17] T. Suksrichavalit, S. Prachayasittikul, C. Nantasenamat, C. Isarankura-Na-Ayudhya, V. Prachayasittikul, Copper complexes of pyridine derivatives with superoxide scavenging and antimicrobial activities., Eur. J. Med. Chem. 44 (2009) 3259–65. doi:10.1016/j.ejmech.2009.03.033.

[18] A. Berahou, A. Auhmani, N. Fdil, A. Benharref, M. Jana, C.A. Gadhi, Antibacterial activity of Quercus ilex bark's extracts., J. Ethnopharmacol. 112 (2007) 426–9. doi:10.1016/j.jep.2007.03.032.

[19] F. Rowe, S. Vargas Superti, R. Machado Scheibe, C.G. Dias, Agar diffusion, agar dilution, Etest®, and agar screening test in the detection of methicillin resistance in staphylococci, Diagn. Microbiol. Infect. Dis. 43 (2002) 45–48. doi:10.1016/S0732-8893(02)00359-0.

[20] C.K. Johnson, ORTEP-II. A Fortran Thermal-Ellipsoid Plot Program, Oak Ridge Natl. Lab. Tennessee, USA. (1976) Report ORNL-5318.

[21] D. Yan, A. Delori, G.O. Lloyd, B. Patel, T. Friscic, G.M. Day, D.-K. Bucar, W. Jones, J. Lu, M. Wei, D.G. Evans, X. Duan, Modification of luminescent properties of a coumarin derivative by formation of multi-component crystals, CrystEngComm. 14 (2012) 5121–5123. doi:10.1039/C2CE25217A.

[22] U.K. Das, V.G. Puranik, P. Dastidar, Supramolecular Synthon Transferability and Gelation by Diprimary Ammonium Monocarboxylate Salts, Cryst. Growth Des. 12 (2012) 5864–5868. doi:10.1021/cg301242p.

[23] G.E. Escudero, C.H. Laino, G.A. Echeverria, O.E. Piro, N. Martini, A.N. Rodriguez, J.J. Martinez Medina, L.L. Lopez Tevez, E.G. Ferrer, P.A.M. Williams, Improving the antidepressant action and the bioavailability of sertraline by co-crystallization with coumarin 3-carboxylate. Structural determination., Chem. Biol. Interact. 249 (2016) 46–55. doi:10.1016/j.cbi.2016.03.010.

[24] J.A.K. Howard, M.F. Mahon, P.R. Raithby, H.A. Sparkes, Trans-cinnamic acid and coumarin-3-carboxylic acid: experimental charge-density studies to shed light on [2+2] cycloaddition reactions, Acta Crystallogr. Sect. B. 65 (2009) 230–237. doi:10.1107/S0108768109001566.

[25] K. Ejsmont, M. Wasielewski, J. Zaleski, Tris(1,10-phenanthroline)zinc(II) dichromate tetrahydrate, Acta Crystallogr. Sect. E Struct. Reports Online. 58 (2002) m200–m202. doi:10.1107/S1600536802006402.

[26] A.J. Dobson, R.E. Gerkin, Coumarin-3-carboxylic Acid, Acta Crystallogr. Sect. C Cryst. Struct. Commun. 52 (1996) 3081–3083. doi:10.1107/S0108270196010852.

[27] K. Nakamoto, Infrared and Raman Spectra of Inorganic and Coordination Compounds, 6th ed., John Wiley & Sons, Inc., Hoboken, NJ, USA, 2008. doi:10.1002/9780470405888.

[28] A. Karaliota, O. Kretsi, C. Tzougraki, Synthesis and characterization of a binuclear coumarin-3-carboxylate copper(II) complex, J. Inorg. Biochem. 84 (2001) 33–37. doi:10.1016/S0162-0134(00)00214-2.

[29] E.M. Layton, R.D. Kross, V.A. Fassel, Correlation of Bond Length with Stretching Frequency for Carbon-Oxygen and Carbon-Nitrogen Systems, J. Chem. Phys. 25 (1956) 135–138. doi:10.1063/1.1742805.

[30] A.A. Schilt, R.C. Taylor, Infra-red spectra of 1:10-phenanthroline metal complexes in the rock salt region below 2000 cm^{-1}, J. Inorg. Nucl. Chem. 9 (1959) 211–221. doi:10.1016/0022-1902(59)80224-4.

[31] T.P. Gerasimova, S.A. Katsyuba, Bipyridine and phenanthroline IR-spectral bands as indicators of metal spin state in hexacoordinated complexes of Fe(II), Ni(II) and Co(II), Dalt. Trans. 42 (2013) 1787–1797. doi:10.1039/C2DT31922E.

[32] Y. Cui, Q. Gao, H.-H. Wang, L. Wang, Y.-B. Xie, Diaqua-bis-(2-oxo-2H-chromene-3-carboxyl-ato)copper(II)., Acta Crystallogr. Sect. E. Struct. Rep. Online. 67 (2011) m782. doi:10.1107/S1600536811018708.

[33] Y. Cui, Q. Gao, H.-H. Wang, L. Wang, Y.-B. Xie, Diaquabis(2-oxo-2H-chromene-3-carboxylato-κ^2O^2,O^3)manganese(II), Acta Crystallogr. Sect. E Struct. Reports Online. 67 (2011) m727–m727. doi:10.1107/S1600536811016667.

[34] Y. Cui, Q. Gao, H.-H. Wang, L. Wang, Y.-B. Xie, Diaqua-bis-(2-oxo-2H-chromene-3-carboxyl-ato-κ^2O^2,O^3)cadmium, Acta Crystallogr. Sect. E Struct. Reports Online. 67 (2011) m126–m126. doi:10.1107/S1600536810053523.

[35] G. Brahmachari, Room Temperature One-Pot Green Synthesis of Coumarin-3- carboxylic Acids in Water: A Practical Method for the Large-Scale Synthesis, Sustain. Chem. Eng. 3 (2015) 2350–2358. doi:10.1021/acssuschemeng.5b00826.

[36] D. Vyprachticky, D. Kankova, V. Pokorna, I. Kmınek, V. Dzhabarov, V. Cimrova, Novel and Simple Synthesis of Brominated 1,10-Phenanthrolines, Aust. J. Chem. 67 (2014) 915–921. https://doi.org/10.1071/CH13711.

[37] G.D. Dimitrov, M.S. Atanassova, Synthesis and Spectroscopic Characterization of a Complex of 1, 10-Phenanthroline with Magnesium, Zeitschrift Für Anorg. Und Allg. Chemie. 629 (2003) 12–14. doi:10.1002/zaac.200390005.

[38] E. Wojaczynska, J. Skarzewski, L. Sidorowicz, R. Wieczorek, J. Wojaczynski, Zinc complexes formed by 2,2[prime or minute]-bipyridine and 1,10-phenanthroline moieties combined with 2-azanorbornane: modular chiral catalysts for aldol reactions, New J. Chem. 40 (2016) 9795–9805. doi:10.1039/C6NJ02251K.

[39] L. Pazderski, T. Pawlak, J. Sitkowski, L. Kozerski, E. Szłyk, ^{1}H NMR assignment corrections and ^{1}H, ^{13}C, ^{15}N NMR coordination shifts structural correlations in Fe(II), Ru(II) and Os(II) cationic complexes with 2,2′-bipyridine and 1,10-phenanthroline, Magn. Reson. Chem. 48 (2010) 450–457. doi:10.1002/mrc.2600.

[40] S. Lin, T. Hong, J. Tung, J. Chen, Molecular Structures of Ge(tpp)$(OAc)_2$ and In(tpp)(OAc) and Their Implications: Correlations between the ^{13}C NMR Chemical Shift of the Acetato Ligand and Different Types of Carboxylate Coordination in M(por)$(OAc)_n$, Inorg. Chem. 36 (1997) 3886–3891. doi:10.1021/ic961304i.

[41] I. Georgieva, I. Kostova, N. Trendafilova, V.K. Rastogi, W. Kiefer, DFT, IR, Raman and NMR study of the coordination ability of coumarin-3-carboxylic acid to Pr(III), J. Mol. Struct. 979 (2010) 115–121. doi:10.1016/j.molstruc.2010.06.013.

[42] S. Yamamura, H. Gotoh, Y. Sakamoto, Y. Momose, Physicochemical properties of amorphous salt of cimetidine and diflunisal system, Int. J. Pharm. 241 (2002) 213–221. doi:10.1016/S0378-5173(02)00195-3.

[43] M.I. Azócar, M. Aldabaldetrecu, P. Levin, L. Tamayo, J. Guerrero, M.A. Páez, Correlating light and thermal stability of silver carboxylate complexes by infrared and ^{13}C NMR spectroscopy, J. Coord. Chem. 69 (2016) 3472–3479. doi:10.1080/00958972.2016.1234610.

[44] R.L. Dean, Kinetic studies with alkaline phosphatase in the presence and absence of inhibitors and divalent cations, Biochem. Mol. Biol. Educ. 30 (2002) 401–407. doi:10.1002/bmb.2002.494030060138.

[45] K.C. Chan, S. Ho, J. Law, V. Yuen, The Effects of Various Divalent Cations on the Enzyme Activity of Bovine Intestinal Alkaline Phosphatase, J. Exp. Microbiol. Immunol. 2 (2002) 13–21. https://www2.microbiology.ubc.ca/sites/default/files/roles/drupal_ungrad/JEMI/2/2-13.pdf.

[46] M. Li, W. Ding, B. Baruah, D.C. Crans, R. Wang, Inhibition of protein tyrosine phosphatase 1B and alkaline phosphatase by bis(maltolato)oxovanadium (IV)., J. Inorg. Biochem. 102 (2008) 1846–53. doi:10.1016/j.jinorgbio.2008.06.007.

[47] D.J. Plocke, B.L. Vallee, Interaction of Alkaline Phosphatase of E. coli with Metal Ions and Chelating Agents, Biochemistry. 1 (1962) 1039–1043. doi:10.1021/bi00912a014.

[48] M. Bortolato, F. Besson, B. Roux, Role of metal ions on the secondary and quaternary structure of alkaline phosphatase from bovine intestinal mucosa, Proteins Struct. Funct. Genet. 37 (1999) 310–318. doi:10.1002/(SICI)1097-0134(19991101)37:2<310::AID-PROT16>3.0.CO;2-B.

[49] N.M. Urquiza, M. Soledad Islas, M.L. Dittler, M.A. Moyano, S.G. Manca, L. Lezama, T. Rojo, J.J. Martínez Medina, M. Diez, L. López Tévez, P.A.M. Williams, E.G. Ferrer, Inhibition behavior on alkaline phosphatase activity, antibacterial and antioxidant activities of ternary methimazole–phenanthroline–copper(II) complex, Inorganica Chim. Acta. 405 (2013) 243–251. doi:10.1016/j.ica.2013.05.022.

[50] J.C.A. Tanaka, C.C. da Silva, A.J.B. de Oliveira, C.V. Nakamura, B.P. Dias Filho, Antibacterial activity of indole alkaloids from Aspidosperma ramiflorum, Brazilian J. Med. Biol. Res. 39 (2006) 387–391. doi:10.1590/S0100-879X2006000300009.

[51] A.A. Aliero, A.D. Ibrahim., Salmonella - A Diversified Superbug, InTech, Croatia, 2012. doi:10.5772/2471.

[52] L.L. López Tévez, M.S. Islas, J.J.M. Medina, M. Diez, O.E. Piro, E.E. Castellano, E.G. Ferrer, P.A.M. Williams, Structural, spectral and potentiometric characterization, and antimicrobial activity studies of $[Zn(phen)_2(cnge)(H_2O)](NO_3)_2.H_2O$, J. Coord. Chem. 65 (2012) 2304–2318. doi:10.1080/00958972.2012.693175.

[53] S. Roy, K.D. Hagen, P.U. Maheswari, M. Lutz, A.L. Spek, J. Reedijk, G.P. van Wezel, Phenanthroline derivatives with improved selectivity as DNA-targeting anticancer or antimicrobial drugs., ChemMedChem. 3 (2008) 1427–1434. doi:10.1002/cmdc.200800097.

[54] M. Mujahid, N. Trendafilova, A.F. Arfa-Kia, G. Rosair, K. Kavanagh, M. Devereux, M. Walsh, S. McClean, B.S. Creaven, I. Georgieva, Novel silver(I) complexes of coumarin oxyacetate ligands and their phenanthroline adducts: Biological activity, structural and spectroscopic characterisation, J. Inorg. Biochem. 163 (2016) 53–67. doi:10.1016/J.JINORGBIO.2016.07.010.

[55] B.S. Creaven, D.A. Egan, D. Karcz, K. Kavanagh, M. McCann, M. Mahon, A. Noble, B. Thati, M. Walsh, Synthesis, characterisation and antimicrobial activity of copper(II) and manganese(II) complexes of coumarin-6,7-dioxyacetic acid ($cdoaH_2$) and 4-methylcoumarin-6,7-dioxyacetic acid ($4\text{-}MecdoaH_2$): X-ray crystal structures of $[Cu(cdoa)(phen)_2]$, J. Inorg. Biochem. 101 (2007) 1108–

1119. doi:10.1016/j.jinorgbio.2007.04.010.

[56] S.B. Kalia, G. Kaushal, M. Kumar, S.S. Cameotra, A. Sharma, M.L. Verma, S.S. Kanwar., S.S. Kanwar, Antimicrobial and toxicological studies of some metal complexes of 4-methylpiperazine-1-carbodithioate and phenanthroline mixed ligands, Braz. J. Microbiol. 40 (2009) 916–922. doi:10.1590/S1517-838220090004000024.

[57] N. Ndosiri, M. Agwara, A. Paboudam, P. Ndifon, D. Yufanyi, C. Amah, Synthesis, characterization and antifungal activities of Mn(II), Co(II), Cu(II), and Zn(II) mixed-ligand complexes containing 1,10 - phenanthroline and 2,2`-bipyridine., Res. J. Pharm. Biol. Chem. Sci. 4 (2013) 386. https://www.rjpbcs.com/pdf/2013_4(1)/[43].pdf.

[58] X.-Z. Wu, D. Chen, L.-S. Zhao, X.-H. Yu, M. Wei, Y. Zhao, Q. Fang, Q. Xu, Early diagnosis of bacterial and fungal infection in chronic cholestatic hepatitis B, World J. Gastroenterol. 10 (2004) 2228. doi:10.3748/wjg.v10.i15.2228.

Table 1. Crystal data and structure refinement results for $[Zn(phen)_3](CCA)(NO_3).xH_2O$.

Empirical formula	$C_{46}H_{29}N_7O_7Zn$	
Formula weight	857.13	
Temperature	297(2) K	
Wavelength	0.71073 Å	
Crystal system	Triclinic	
Space group	$P\bar{1}$	
Unit cell dimensions	a = 12.3818(5) Å	α = 113.768(3)°
	b = 15.1143(4) Å	β = 112.826(4)°
	c = 15.4875(6) Å	γ = 90.329(3)°
Volume	2399.25(17) $Å^3$	
Z	2	
Density (calculated)	1.186 Mg/m^3	
Absorption coefficient	0.564 mm^{-1}	
F(000)	880	
Crystal size	0.282 x 0.218 x 0.135 mm^3	
ϑ-range for data collection	3.206 to 29.449°	
Index ranges	$-16 \le h \le 16$, $-18 \le k \le 18$, $-18 \le l \le 21$	
Reflections collected	21439	
Independent reflections	10998 [R(int) = 0.036]	
Observed reflections	7408	
Completeness to ϑ = 25.242°	99.8 %	
Refinement method	Full-matrix least-squares on F^2	
Data / restraints / parameters	10998 / 0 / 514	
Goodness-of-fit on F^2	1.015	
Final R indices [I>2sigma(I)]	R1 = 0.0572, wR2 = 0.1629	
R indices (all data)	R1 = 0.0878, wR2 = 0.1836	
Largest diff. peak and hole	0.415 and -0.375 $e.Å^{-3}$	

[a] $R_1=\Sigma||F_o|-|F_c||/\Sigma|F_o|$, $wR_2=[\Sigma w(|F_o|^2-|F_c|^2)^2/\Sigma w(|F_o|^2)^2]^{1/2}$

Table 2. Main vibrational modes observed by FTIR and Raman (bold) of different compounds with Zn(II), HCCA and phen

Assignment	HCCA	KCCA	ZnCCA	phen	ZnCCAphen	Znphen
ν OH (H_2O)			3221 (br)	3408 (br)	3336 (br) 3261 (br)	3389 (br)
ν OH (bridge)	2933 (s)					
ν C=O (carboxylic)	1744 (s) **1738 (m)**					
ν C=O (carbonyl)	1682 (s) **1680 (w)**		1669 (s) **1675 (m)**		1670 (s) **1675 (w)**	1733 (s) **1738 (m)**
ν C=C	1609 (s) **1615 (s)**	1627 (s) **1627 (s)**	1616 (s)		1625 (s) **1627 (s)**	1624 (s) **1625 (s)**
		1608 (sh) **1609 (s)**	1609 (m) **1609 (s)**		1598 (sh) **1606 (s)**	1607 (sh) **1608 (s)**
ν_{as} COO		1597 (s) **1599 (sh)**	1563 (m) **1567 (m)**		1563 (s) 1555 (s) **1560 (w)**	1596 (m) **1589 (m)**
ν_s COO		1391 (sh) **1396 (m)**	1367 (w) **1369 (m)**		1367 (m) **1369 (m)**	
ν_s COO + ν_3 NO_3						1384 vs, br **1422 vs (phen)** **1377 w**
ν_1 NO_3						**1057 s**
o-phen				853 (s) **855 (w)**	850 (s)	847 (s)
o-phen				738 (s)	725 (s) **729 (s)**	724 (s) **723 (sh)**

Abbreviations: vs, very strong; s, strong; m, medium; w, weak; sh, shoulder; br, broad. ν, stretching; s, symmetric; as, antisymmetric.

Table 3. Comparison of bond lengths and vibrational stretchings for CO (carbonyl, carboxylic acid and carboxylate) groups.

	HCCA [a]		**ZnCCA** [b]		**Znphen**	
	Bond length (Å)	ν C=O (cm^{-1})	Bond length (Å)	ν C=O (cm^{-1})	Bond length (Å)	ν C=O (cm^{-1})
C=O (carboxylic)	1.199	1744 (s)				
CO (carboxylate)			1.245 1.264	1561 1396	1.245 1.268	1596 1384
C=O (carbonyl)	1.216	1682 (s)	1.232	1669 (s)	1.199	1733 (s)

[a] Crystallographic data for HCCA obtained from [26]; [b] Crystallographic data measured in this work for comparison with data obtained by Y. Cui et al. [10].

Table 4. Comparison of CO bond lengths for the carbonyl, carboxylic and carboxylate groups.

	HCCA [26]	CuCCA [32]	MnCCA [33]	CdCCA [34]	ZnCCA [10]	ZnCCA[a]	CCA[a] anion
C=O carbonyl	1.216	1.216	1.222	1.227	1.2241	1.232	1.199
C=O carbox	1.199	1.251 1.266	1.2509 1.2549	1.256 1.257	1.2501 1.2617	1.245 1.264	1.245 1.268
C-O(H) carbox	1.328						

[a] Crystallographic data measured in this work and [b] for comparison with data obtained by Y. Cui et al. [10].

Table 5: ^{1}H and ^{13}C NMR main chemical shifts in DMSO-d_6 of HCCA, KCCA and binary and ternary complexes of Zn(II).

	Group	HCCA		KCCA		ZnCCA		ZnCCAphen		phen [38]	
		^{1}H	^{13}C	^{1}H	^{13}C	^{1}H	^{13}C	^{1}H	^{13}C	^{1}H	^{13}C
CCA	C(3)OOH	13.25 (s)	164	-	165	-	167	-	167		
	C(1)=O	-	157	-	153	-	158	-	158		
	CH (4)	8.76 (s)	149	7.82 (s)	137	8.53 (s)	145	8.15 (s)	143		
	CH (7)	7.92 (d)	130	7.67 (d)	128	7.85 (d)	130	7.64 (d)	129		
	CH(10)	7.74 (t)	135	7.50 (t)	130	7.65 (t)	133	7.57 (t)	133		
	CH(8)	7.44 (m)	116	7.29 (m)	116	7.39 (m)	116	7.28 (m)	116		
	CH(9)	7.42 (m)	125	7.27 (m)	124	7.36 (m)	125	7.27 (m)	125		
phen	CH(2)	-		-		-		8.78 (br)	139	9.18	150.4
	CH(3)	-		-		-		7.25 (br)	129	7.62	123.1
	CH(4)	-		-		-		8.18 (br)	127	8.23	136.0
	CH(6)	-		-		-		7.93 (br)	125	7.77	126.6

Chemical shifts are expressed in ppm using TMS as reference. In parentheses the signal multiplicities are indicated (s: singlet, d: doublet, t: triplet, m: multiplet, br: broad).

Table 6. Minimum inhibitory concentration (MIC) of metal Zn(II), free ligands (phen and HCCA), binary complex ZnCCA and ternary complex ZnCCAphen for fungus and bacteria reference strains, in μg mL^{-1}. Minimum inhibitory concentration (MIC, μg mL^{-1}): Inactive (above 1000), weak toxicity (1000-500), moderate (500-100), significant toxicity (lower than 100). Minimum values are shown in bold.

		Zn(II)	phen	HCCA	ZnCCA	ZnCCAphen
Bacteria	*P. aeruginosa*	1500	375	1500	>1500	>1500
	E. faecalis	1500	**94**	1500	>1500	1500
	E. coli	188	**12**	>1500	>1500	1500
	S. aureus	188	**24**	1500	>1500	750
	S. epidermidis	188	**12**	1500	1500	750
Fungi	*C. albicans* ATCC 10231	1500	**3**	>1500	>1500	**12**
	C. glabrata	1500	**6**	>1500	>1500	**24**
	C. krusei	1500	**6**	>1500	>1500	**24**
	C. parapsilosis ATCC 22019	750	**12**	>1500	>1500	**188**
	C. tropicalis	750	**12**	>1500	>1500	**188**

Graphical abstract

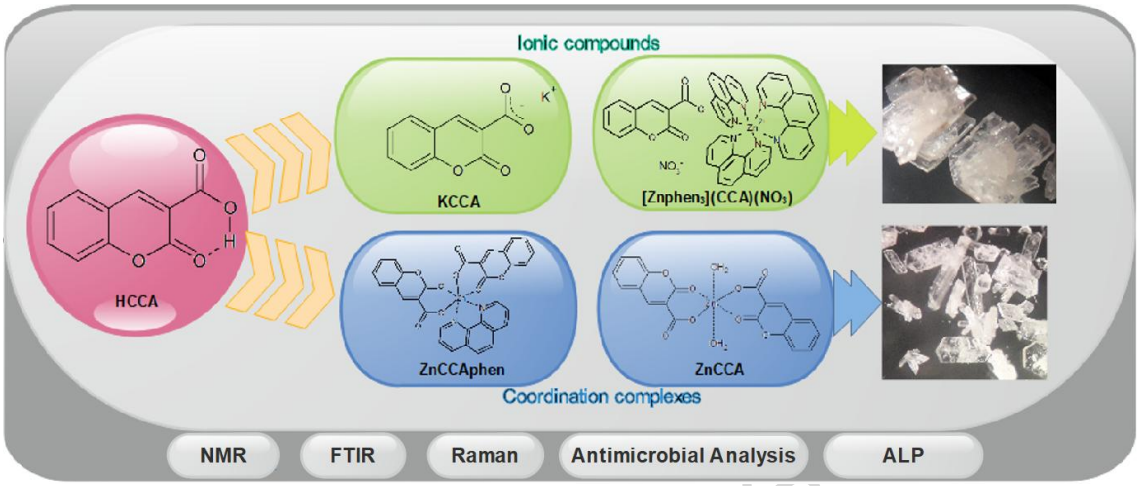

Highlights

- ✓ Zn coumarin-3-carboxylate o-phenanthroline compounds
- ✓ Vibrational determinations based in bond length
- ✓ NMR characterization
- ✓ Antimicrobial activities and behavior against alkaline phosphatase